

Ideal gas of vortices in type-II superconductors: Experiment and theoretical model.

V. Kozhevnikov¹, A.-M. Valente-Feliciano², P. J. Curran³, G. Richter⁴,
A. Volodin⁵, A. Suter⁶, S. Bending³ and C. Van Haesendonck⁵

¹*Tulsa Community College, Tulsa, Oklahoma 74119, USA*

²*Thomas Jefferson National Lab, Newport News, VA 23606, USA*

³*University of Bath, Bath BA2 7AY, United Kingdom*

⁴*Max-Planck-Institut für Intelligent Systems, 70569 Stuttgart, Germany*

⁵*Solid State Physics and Magnetism Section, KU Leuven, BE-3001 Leuven, Belgium*

⁶*Paul Scherrer Institut, 5232 Villigen PSI, Switzerland*

Equilibrium magnetic properties of the mixed state in type-II superconductors were measured with high purity bulk and film niobium samples in parallel and perpendicular magnetic fields using dc magnetometry and scanning Hall-probe microscopy. Equilibrium magnetization data for the perpendicular geometry were obtained for the first time. It was found that none of the existing theories is consistent with these new data. To address this problem, a theoretical model is developed and experimentally validated. The new model describes the mixed state in an averaged limit, i.e. ignoring interactions between vortices. It is quantitatively consistent with the data obtained in a perpendicular field and provides new insights on properties of vortices. At low values of the Ginzburg-Landau parameter, the model converts to that of Peierls and London for the intermediate state in type-I superconductors. It is shown that description of the vortex matter in superconductors in terms of a 2D gas is more appropriate than the frequently used crystal- and glass-like scenarios.

PACS numbers:

INTRODUCTION

Magnetic properties of type-II superconductors in the mixed state (MS) are discussed in all superconductivity textbooks and in numerous papers following after fundamental experiments of Shubnikov and coworkers [1], where type-II superconductivity was discovered. References for many of these papers can be found, e.g., in [2–4]. Therefore, it may be quite surprising that *far* not all, including the most basic, magnetic properties are known. Examples include, but are not limited to, a magnetization curve $M(H)$, where M is magnetic moment and H is the applied field, and the field strength $H^{(i)}$ (also referred as the magnetic force [5], the thermodynamic field [6], and the Maxwell field [7]) in samples of other than cylindrical geometry. We will use this term for infinite cylinders and slabs in a parallel field, i.e. for samples with demagnetizing factor $\eta = 0$ [8].

Here we present experimental results on equilibrium magnetic properties of the MS measured with high purity niobium samples in parallel and perpendicular magnetic fields. To the best of our knowledge such data for the perpendicular field were not available earlier. A theoretical model quantitatively accounting for the new data is developed and introduced here as well. Similar to a model of Peierls [9] and London [10, 11] for the intermediate state (IS) of type-I superconductors, the new model describes the MS in an averaged limit, that is without detailing the samples' magnetic structure and therefore ignoring interactions between the structural units (vortices). At low values of the Ginzburg-Landau (GL) parameter κ , the new model converts to that of Peierls and

London for the intermediate state (IS) of type-I superconductors, valid in the limit of non-interacting normal domains [15]. Overall, the new model accounts for equilibrium magnetic properties of all (known) superconductors of any ellipsoidal shape ($0 \leq \eta \leq 1$) in a zero-order approximation. We will show that description of the vortex matter as a 2D gas of noninteracting vortices is the most appropriate for samples of a transverse geometry. The latter term will be used for the infinite slabs or films in a perpendicular magnetic field, i.e. for samples with $\eta = 1$.

PROBLEM STATUS AND MOTIVATION

There are two equilibrium superconducting states where samples consist of domains of normal (N) and superconducting (S) phases. Those are the IS in type-I and the MS in type-II materials. In the IS, due to positive energy of the S-N interface, the N domains are multi flux quantum laminae, whereas in the MS, due to negative sign of this energy, these domains are single flux quantum vortices. This quantitative difference in the flux magnitude results in drastic qualitative differences in properties of type-I and type-II superconductors. In particular, the MS takes place in samples of any shape including cylindrical one (i.e. for $0 \leq \eta \leq 1$), whereas the IS occurs only if $\eta \neq 0$ [12]. (Under "shapes" we mean shapes of ellipsoids, because only ellipsoids allow performing rigorous theoretical treatment of the magnetic properties [5].)

Due to that, significant attention was paid to measurements of the magnetization with cylindrical samples, which, in particular, led to a fairly good knowledge of the $M(H)$ curve for this geometry [1, 3, 13, 14].

For cylinders at $H < H_{c1}$ the Meissner condition $B = 0$ allows one to calculate $M(H)$ from either thermodynamics, or magnetostatics (see, e.g. [15]), or the Maxwell field $H^{(i)} (= H$ in this case). Recall that $H^{(i)}$ is defined as $B - 4\pi m$, where B is the induction and m is magnetization, which for uniform samples of volume V is M/V .

However in the MS complexity of current distribution leaves only one option to calculate M , i.e. through the field $H^{(i)}$ via calculation of an average induction \bar{B} . For cylinders this was done using the GL theory (valid near the critical temperature T_c [16, 17]) near H_{c1} and H_{c2} [12], and also with use of the London equation for the vicinity of H_{c1} [7, 17]. Approximate analytical expressions for \bar{B} are available for $\ln \kappa \gg 1$ [7, 12, 17]. At the same time it is supposed that entire $M(H)$ curve for any κ can be calculated via numeral solution of the GL equations [18]. Note however, that an approximate solution of these equations (different from the exact solution for $< 5\%$) is not quite consistent with this supposition, e.g. a jump of M at H_{c1} increases with increasing κ [19], whereas in experiment [13] this jump decreases.

The situation is greatly complicated for non-cylindrical geometry. For the experiments, it is due to a much larger number of pinning centers in the sample area perpendicular to the field. On that reason available data on $M(H)$ for the MS in the transverse geometry (see, e.g., [20–22]) are strongly irreversible and, therefore, inappropriate for judgment on thermodynamic properties.

On the theoretical side, the main complication is due to a demagnetizing field $\mathbf{H}^{(d)} \equiv \mathbf{H} - \mathbf{H}^{(i)}$. The Maxwell field $H^{(i)}$ in homogeneous ellipsoids is uniform but different from H [2, 5, 8]. If H is parallel to the sample axis, relative to which the demagnetizing factor is η , then

$$(1 - \eta)H^{(i)} + \eta B = H. \quad (1)$$

Therefore

$$H^{(i)} \equiv H - H^{(d)} = H - \eta(B - H^{(i)}) = H - \eta 4\pi m. \quad (2)$$

Thus, in uniform samples, $H^{(d)} = 4\pi\eta m$. In the Meissner state the sample is homogeneous, which, together with condition $B = 0$, allows one to calculate $H^{(i)}$ from Eq. (1) and then M from Eq. (2) in full consistency with experiments (see, e.g., [2]). However this is not the case for the MS, where the sample is not uniform and therefore η is not defined and neither $H^{(d)}$, nor $H^{(i)}$ are known.

Here one can probably object by saying that there is a well known approach [6, 23] in which $H^{(i)}$ for $\eta \neq 0$ is calculated from Eq. (1), then \bar{B} is calculated using $\bar{B}(H)$ obtained for the cylindrical geometry (referred as $B_e(H)$) replacing H by $H^{(i)}$, and then both $B_e(H^{(i)})$ and $H^{(i)}$ are used to calculate M . However, at $\eta = 1$, where $\bar{B} = H$, Eq. (1) becomes $H^{(i)}(1 - 4\pi) = H(1 - 4\pi)$ thus yielding $H^{(i)} = H$ and therefore $M = 0$ regardless on H , meaning that $H_{c2} = \infty$. A reason of such a striking inadequacy of this approach (apart from an error in [6]) is very simple: Eq. (1) is inapplicable for inhomogeneous samples. A uniform sample with $\eta = 1$ is just a sample in the N state where M is indeed zero.

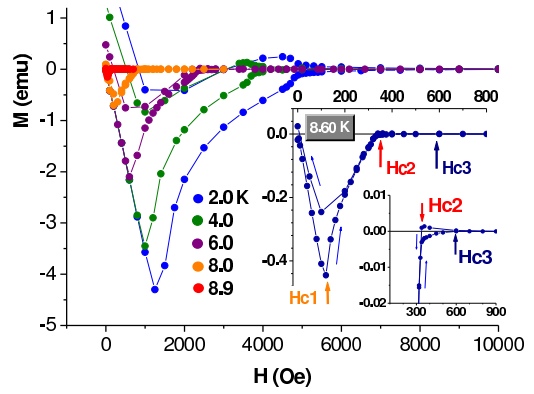


FIG. 1: Data on the magnetic moment of Nb-SC sample measured in the parallel field at temperatures indicated in the figure. Inserts: M vs H at $T = 8.60$ K in two scales.

In [24, 25] $M(H)$ for films with different κ and d in the perpendicular field was calculated using the GL theory. Calculated curves strongly depend on κ and d , but contradict the rule-of-1/2 [15] (see more about this rule below) and hence are irrelevant.

The approach employing the London equation [17] does not work for the transverse geometry either. The reason is that, in the cylinders, the thermodynamic potential $\tilde{F} \equiv F - BH^{(i)}/4\pi = F - BH/4\pi$ is minimized exclusively for the expense of the second term, reflecting the work done by the magnet power supply when the flux through the sample changes. Here F is the Helmholtz potential and \tilde{F} is its Legendre transform, often referred as the Gibbs free energy [11]. In the transverse geometry, the flux is fixed and hence the term $BH^{(i)}/4\pi$ is absent, making the minimization of $\tilde{F} = F$ impossible.

After all, inhomogeneities of the field and of the vortex cores near the sample surface should be taken into account. These inhomogeneities, unimportant when $\eta = 0$, can be important for films in nonparallel fields making their properties dependent on the film thickness. For instance, in the IS they can change the critical field of a few μm thick film in the perpendicular field for more than 50% compare to that in the parallel field [15, 26]. An attempt to address this issue for the MS was interpreted by Cody and Miller in experiments with lead films [22], however the results obtained are inconclusive due to strong pinning in their films.

To summarize, (a) available experimental information on the magnetic properties of the MS in non-cylindrical samples is incomplete. In particular, magnetization data are strongly irreversible and hence inapplicable for thermodynamic consideration and guiding the theory. (b) Available theoretical results and approaches are controversial. In particular, none of the existing theories is capable to address the properties of samples with $\eta = 1$. Progress toward solution of this fundamental problem is the goal of our work, which results are presented below.

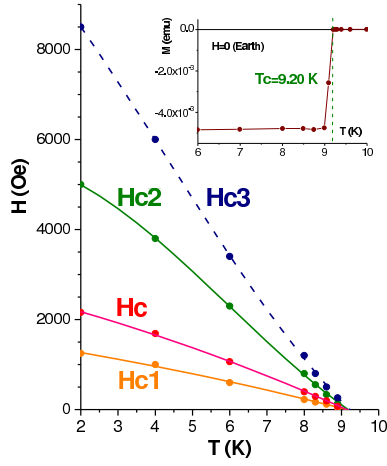


FIG. 2: Phase diagram of the single crystal sample Nb-SC. H_{c1} , H_c , H_{c2} and H_{c3} indicate the graphs for the respective critical fields. Insert: magnetic moment measured at zero (Earth) field versus temperature.

EXPERIMENTAL

Fabrication of the pinning free samples, being very challenging for type-I materials [2, 15], is even more difficult for type-II superconductors, since most of them are alloys with inevitably significant pinning [1, 6]. A single crystal sample is a solution, but since we also need a film for verification of dependencies of the properties on the sample thickness, such a solution is not complete.

Nb is known as a well verified intrinsic type-II superconductor [14, 27], hence it is a material from which one can hope to fabricate the pinning free films. On this reason Nb was chosen for our samples. However Nb is also known as a getter [14]. Due to that, our first films, deposited via magnetron sputtering and having residual resistivity ratio $RRR \approx 70$, were still insufficiently clean.

A Nb film sample (Nb-F) used in this work was grown on sapphire via Electron cyclotron resonance technique (ECR) [28]; its $RRR = 640$, the size is $4 \times 6 \text{ mm}^2$ and $d = 5.7 \mu\text{m}$. This is a record pure niobium film, of the same purity as indium films in studies of the IS [15, 26]. More about ECR grown Nb films can be found in [29].

Another sample (Nb-SC) was a single crystal Nb provided by Surface Preparation Laboratory, Netherlands. It was a one side polished disc $\varnothing 7 \text{ mm} \times 1 \text{ mm}$.

However there is one more issue with Nb samples. A driving force to achieve thermodynamic equilibrium in inhomogeneous samples is the S-N surface tension [15], which magnitude in type-II Nb is significantly less than that in type-I In. This could require even more pure Nb samples, but fortunately pinning weakens with temperature T . Specifically, both our samples are close to pinning-free at $T \gtrsim 8 \text{ K}$. For this reason, we mostly discuss the data obtained at high temperatures.

The magnetic moment was measured using Quantum Design MPMS system. Data obtained with Nb-SC sample in the parallel field are shown in Fig. 1 with typi-

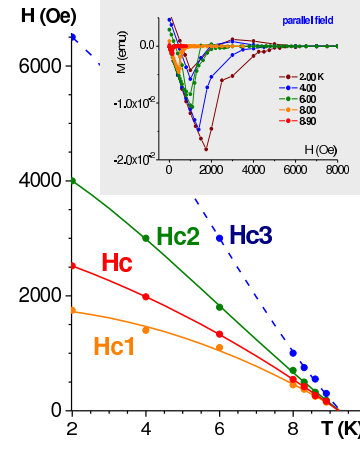


FIG. 3: Phase diagram of the film sample Nb-F. H_{c1} , H_c , H_{c2} and H_{c3} indicate the graphs for the respective critical fields. Insert: experimental data on the sample magnetic moment measured in parallel field at indicated temperatures under ascending and descending field.

cal high-temperature data shown in the inserts. At the Meissner state, all data agree with each other. Hence the sample was well aligned with the field and the flux trapped at the ascending field was low, which allows to calculate the thermodynamic critical field H_c [13]. A sample volume calculated from $M(H)$ in the Meissner range agrees with that measured directly within 5% error, indicating that $\eta_{\parallel} \sim 10^{-2}$ and therefore $\eta_{\perp} (=1-2\eta_{\parallel})$ is close to unity [8]. Here η_{\parallel} and η_{\perp} are the demagnetizing factors in the parallel and the perpendicular fields.

The phase diagram of Nb-SC sample is shown in Fig. 2 with the data for M vs T at Earth field shown in the insert. T_c of this sample is 9.20 K; κ ($=H_{c2}/\sqrt{2}H_c$ [12]) is 1.3 near T_c and up to 1.6 at 2 K.

The phase diagram of Nb-F sample is shown in Fig. 3, where the original magnetization data are shown in the insert. The sample volume was determined from the slope of $M(H)$ at the Meissner state; its uncertainty is 10%. $T_c = 9.25 \text{ K}$ and κ is 0.8 near T_c up to 1.1 at 2 K.

Experimental data for the magnetic moment obtained with Nb-SC and Nb-F samples in the perpendicular field at high temperatures are shown in Figs. 4 and 5, respectively. The data are reversible over more than half of the field range of the MS. Therefore, in this diapason, the sample is in the equilibrium state. The equilibrium $M(H)$ is linear, and its extrapolation (shown by the dash-dot green line) to $H = 0$ yields $4\pi M(0)/V$ close to $-H_{c1}$ (shown by the red star). The validity of such an extrapolation is supported by the rule-of-1/2: the area above the green line equals to the condensation energy $H_c^2 V / 8\pi$ ($=1/2$ in coordinates $4\pi M / H_c V$ vs H / H_c), calculated from the data obtained in the parallel field.

Comparing Figs. 4 and 5 with Figs. 4 and 5 in [15], one can notice a striking similarity in $M(H)$ for the MS and the IS. However there are also important differences: in the IS $M(0)/V$ and the critical field strongly depend

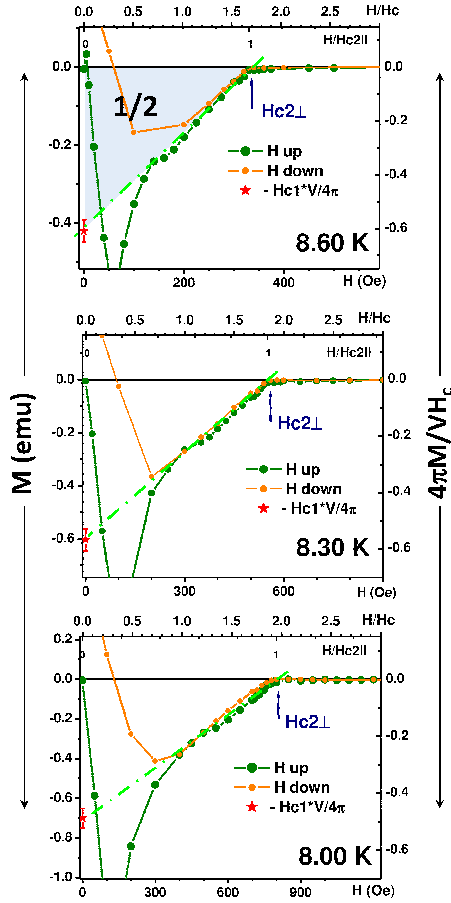


FIG. 4: Magnetic moment of Nb-SC sample measured in the perpendicular field at indicated temperatures. The star shows $M(0) = -H_{c1}V/4\pi$ or $4\pi M(0)/V = -H_{c1}$. Left and right vertical scales show M in different units as indicated; horizontal scales show applied field in Oe (bottom), in units of $H_{c2||}$ (low top) and in units of H_c (upper top). 1/2 is the area above the green line in coordinates $4\pi M/H_cV$ vs H/H_c .

on the sample thickness, whereas for both our samples $4\pi M(0)/V$ is close to $-H_{c1}$ and $H_{c2\perp} = H_{c2||}$, where $H_{c2\perp}$ and $H_{c2||}$ are the critical fields in the perpendicular and the parallel geometries, respectively. Nevertheless, it was important to ensure that our samples are indeed type II superconductors. The most directly it can be done measuring the flux in N domains.

In the MS $\bar{B} = n\Phi_0$ [7], where a planar density $n = N/A$ is a number of flux lines N passing through the area A . In the transverse geometry $\bar{B} = H$ and therefore

$$n = H/\Phi_0. \quad (3)$$

Hence, $n(H)$ allows one to determine the flux in the N domains and therefore the type of a superconductor.

With this in mind we probed the film sample with a scanning Hall-probe microscope (SHPM) [30]. The scanned area was $7.6 \mu\text{m} \times 7.6 \mu\text{m}$. To achieve better resolution determined by a contrast of the field inside and outside the flux lines, the SHPM images were taken at

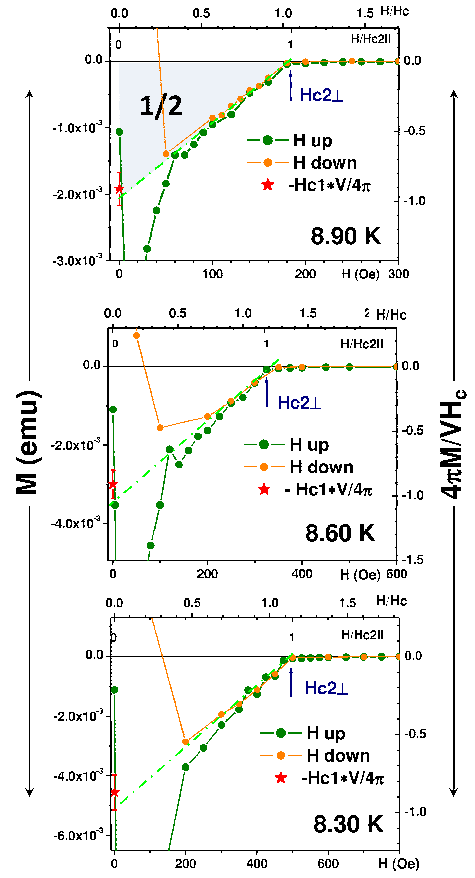


FIG. 5: Magnetic moment of Nb-F sample measured in the perpendicular field at the indicated temperatures. See captions of Fig. 4 for details.

low H . At these fields pinning is not small and therefore the equilibrium triangular structure of the vortex ensemble can be damaged. Typical images taken at $T = 5.0$ and 9.15 K are shown in Fig. 6.

A graph for $n - n_0 = (N - N_0)/A$ vs H is shown in Fig. 7. Here N_0 is an adjustable parameter reflecting occasional number of the lines in the scanned area at Earth field due to pinning and low statistics. As one can see, the experimental points agree with Eq. 3, thus confirming that each flux line carries a single flux quantum Φ_0 . Since κ of our single crystal sample is greater than that of the film, we conclude that our samples are classical type-II superconductors with Abrikosov vortices [12].

THEORETICAL

The problem of the magnetic properties of inhomogeneous superconductors was for the first time addressed by Peierls [9] and F. London [10, 11] for the IS. Both authors solved it in an averaged limit, in which the nonuniform induction B and the magnetization m are replaced by averaged \bar{B} and \bar{m} , respectively. In such a description the demagnetizing factor η is the same as that for the uniform sample. The key element in the Peierls-London model is an assumption that $H^{(i)} = H_c$ in the entire

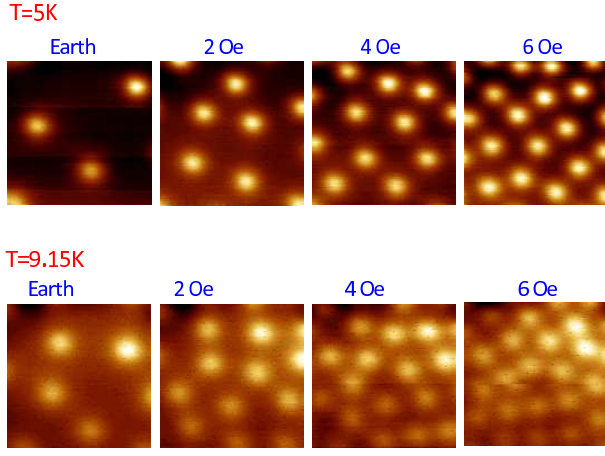


FIG. 6: Scanning Hall-prob images of the MS in Nb film.

range of the IS, justified by a paradigm on instability of the N phase when $H^{(i)} < H_c$. Note, however, that this paradigm is valid only for the cylindrical geometry [26].

The Peierls-London model is valid for thick samples [2, 15, 26], i.e. when the surface related inhomogeneities can be neglected (condition identical to that for the cylindrical geometry). Since N laminae are screened in the sample interior and interact through the outer field, the Peierls-London model represents a global description of the IS in a zero-order approximation, where interaction between the structural units is neglected.

For the MS, such an averaged model is missing, resulting in the absence of the global description of this state and leaving a significant "gap" in understanding the MS magnetic properties. In particular, as shown above, none of the existing theories is capable to address the magnetization curve for a slab in a perpendicular field. A model, presented below, is targeted to fill this gap.

In Fig. 8 graphs for $\eta = 0$ represent the Maxwell field $H^{(i)}$ vs H for the cylindrical geometry. The red section in (b) represents this dependence for the MS, meaning that the function $H^{(i)}(H)$ is linear and extends from H_{c1} to H_{c2} . On the other hand, the experimental results for the transverse geometry (see Figs. 4 and 5), *viz.* (a) linearity of $M(H)$, (b) $H_{c2\perp} = H_{c2\parallel}$ and (c) $4\pi M(0)/V = -H_{c1}$, suggest that $H^{(i)}(H)$ for $\eta = 1$ is also a linear function extending in the same range. Therefore one can assume the linear form of $H^{(i)}(H)$ for all η , as it is shown in Fig. 8b. Analytical expression for these functions is

$$H^{(i)} = H_{c1} + \frac{H_{c2} - H_{c1}}{H_{c2} - H_{c1}(1 - \eta)}[H - H_{c1}(1 - \eta)]. \quad (4)$$

Then from Eq. (2) one obtains for M and \bar{B} :

$$\frac{4\pi M}{V} = -H_{c1} + \frac{H_{c1}}{H_{c2} - H_{c1}(1 - \eta)}[H - H_{c1}(1 - \eta)], \quad (5)$$

$$\bar{B} = \frac{H_{c2}}{H_{c2} - H_{c1}(1 - \eta)}[H - H_{c1}(1 - \eta)]. \quad (6)$$

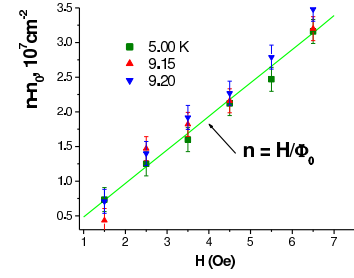


FIG. 7: Dependence of the flux line density on the applied field at different temperatures.

Graphs for these functions are shown in Fig. 9.

In type-I materials, where $H_{c1} = H_{c2} = H_c$, Eq. (4) yields $H^{(i)} = H_c$, as in the Peierls-London model. This is easily seen from Fig. 8b: when $H_{c2} \rightarrow H_{c1}$, meaning that when superconductor converts from type-II to type-I, the graphs in (b) convert to the graphs in (a). Then Eqs. (5) and (6) convert to formulas for M and \bar{B} in the Peierls-London model as well (see [15] for the graphs). Therefore, our model describes averaged properties of both the MS and the IS in the limit of the non-interacting vortices in type-II and laminae in type-I superconductors.

DISCUSSION

First, we briefly stop at the rule-of-1/2 because, being well known (see, e.g. [2]), it is not always clearly articulated in the textbooks. This rule represents the law of the energy conservation in superconductors when \mathbf{M} is aligned (antiparallel) to \mathbf{H} . Consistency with this rule is a prerequisite for discussion of equilibrium properties.

In the general case, this law reads that, at constant T , the total free energy \tilde{F}_M (defined as $\mathbf{M} = -\nabla_{\mathbf{H}} \tilde{F}_M$) of any singly connected superconductor in a dc magnetic field \mathbf{H} of any orientation is

$$\tilde{F}_M(H) = \tilde{F}_M(0) - \int \mathbf{M} d\mathbf{H} = F_{n0} - \frac{H_c^2 V}{8\pi} - \int \mathbf{M} d\mathbf{H}, \quad (7)$$

where F_{n0} is Helmholtz free energy of the N state in zero field. Eq. (7) explicitly shows that, (a) the total free energy in the N state ($= F_{n0}$) is independent on the applied field since magnetic permeability μ of this state is unity, and (b) a source of the magnetic energy E_M of superconductors (the last term in Eq. (7)) is the condensation energy. Finiteness of the latter makes transition to the N state a mandatory property of any superconductor [8].

As one can see from Fig. 9a, the area under the graphs $M(H)$ for different η is the same, meaning that if the magnetic moment is calculated for different orientations of the applied field, the sample condensation energy is the same, as it must be. Therefore our model meets the rule-of-1/2 and we can proceed to discussion.

Comparing the modeled magnetization curve for $\eta = 1$ in Fig. 9a with the experimental data in Figs. 4 and 5, one can see that for the transverse geometry the model is quantitatively consistent with experiment.

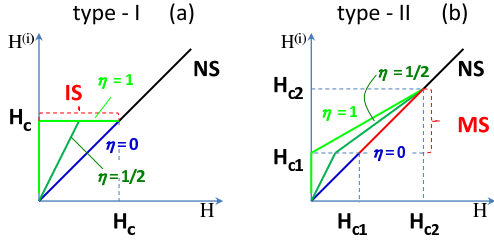


FIG. 8: Maxwell field $H^{(i)}$ in type-I and type-II superconductors of different shapes versus applied field H . Abbreviation: NS, IS and MS designate the normal, intermediate and mixed states, respectively. The demagnetizing factors η are related to a long cylinder in a parallel field ($\eta = 0$), to a long cylinder in a perpendicular field ($1/2$) and to an infinite slab in a perpendicular field (1).

Next, since the area under the graphs in Fig. 9a equal to $H_c^2/2$, we see that H_c is the geometrical mean of H_{c1} and H_{c2} , which is consistent to a rule known for the extreme type-II limit [18]. This suggests that the rule $H_{c1}H_{c2} \approx H_c^2$ is more general than it looked till now.

Further, as shown by Andreev [31], in the IS $H^{(i)}$ is the Maxwell field and hence the induction in the N domains $B_n = \mu H^{(i)}$, since μ of the N phase is unity. Extending this consideration to the MS [17], one can state that $H^{(i)}$ is the Maxwell field in the vortex cores. Therefore our model suggests that B_n in the vortex cores increases from H_{c1} at $H = (1 - \eta)H_{c1}$ to H_{c2} at $H = H_{c2}$ and the structure of individual vortices (in sufficiently thick samples) does not depend on the sample shape (η).

However there is an obvious problem. In Fig. 9 the linear graph $M(H)$ for $\eta = 0$ (cylindrical geometry) differs from the experimental curve, showing a nonlinear increase near H_{c1} (see, e.g., Fig. 1 or [14]). A theoretical description of this feature in $M(H)$ requires accounting interaction between vortices [17]. In our model vortices do not interact, which explains this difference.

A question then arises, whether such a model is needed, if the vortices interact [6, 7, 17, 18]? The same question can be formulated as: Why the experimental graphs $M(H)$ in Figs. 4 and 5 are identical to that in the model of noninteracting vortices in Fig. 9a? A possible answer for the both formulations is: Because in the transverse geometry an interaction between the vortices *vanishes*.

Any superconductor of the transverse geometry passes through the field and optimizes the currents to minimize its magnetic energy and therefore the total free energy \tilde{F}_M . However result of this optimization is radically different in type-I and type-II superconductors. Type-I samples tune a period of the laminar structure, the fraction of the normal phase and induction inside it, as well as the currents and the laminae shape near the surfaces, all together leading to a strong dependence of the magnetic properties on the sample thickness d [15, 26].

No doubts that all these degrees of freedom are also available for type-II superconductors, but owing to the gain received from the negative interface energy, in this

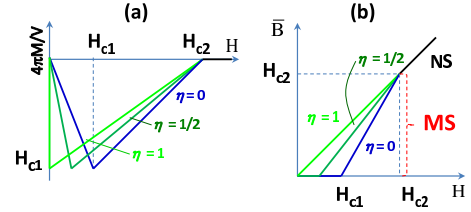


FIG. 9: (a) magnetic moment in and (b) averaged induction of type-II superconductors with different demagnetizing factors η (see caption of Fig. 9 for explanation).

case all tunings are performed keeping maximum possible number of vortices and therefore minimum flux passing through them, i.e. Φ_0 . Then the vortex density n is as that in Eq. (3) and parameter of the most effectively packed triangular vortex lattice $b = (2\Phi_0/\sqrt{3}H)^{1/2}$.

Important that n and b are as such *not* due to the minimization of the free energy F (as it takes place for the same geometry in the IS [26]), but due to the symmetry and the flux conservation and, hence, do not depend on the sample thickness d . Figuratively, choosing Φ_0 for the flux magnitude in the vortices, the sample gives itself to the hands of the supreme power, the symmetry, hence losing control over anything.

On the other hand, as soon as vortices in the transverse geometry do not interact, the sample magnetic energy is a simple sum of the free energies of the individual flux lines ϵd , where ϵ is energy of the line per unit length. Therefore, taking into account that $H = \bar{B} = n\Phi_0 = N\Phi_0/A$ and using Eq.(5) with $\eta = 1$ one obtains

$$E_M = - \int \mathbf{M} d\mathbf{H} = N\epsilon d = \frac{V}{4\pi} H (H_{c1} - \frac{H_{c1}}{2H_{c2}} H) = N d \frac{\Phi_0}{4\pi} (H_{c1} - \frac{H_{c1}}{2H_{c2}} H), \quad (8)$$

which yields

$$\epsilon = \frac{\Phi_0 H_{c1}}{4\pi} (1 - \frac{H}{2H_{c2}}). \quad (9)$$

Comparing ϵ at H_{c1} in the cylindrical geometry ($\Phi_0 H_{c1}/4\pi$ [6, 7, 17, 18]) with Eq.(9), we see that ϵ in the transverse geometry at $H \rightarrow 0$ when $H^{(i)} = H_{c1}$ equals to ϵ in the cylinder, as it must be. At higher field, ϵ decreases becoming $\Phi_0 H_{c1}/8\pi$ at $H=H_{c2}$, where it yields

$$E_M = N\epsilon d = (\frac{H_{c2}A}{\Phi_0}) (\frac{\Phi_0 H_{c1}}{8\pi}) d = \frac{H_{c1}H_{c2}}{8\pi} V = \frac{H_c^2}{8\pi} V, \quad (10)$$

as it must be as well.

Now, we rewrite Eq.(10) as

$$E_M = \frac{H_c^2}{8\pi} N a d = N \frac{H_c^2}{8\pi} v, \quad (11)$$

where a and v are an area and a volume of a unit cell (containing a single flux line), respectively. The latter form

of E_M clearly indicates that the thermodynamic critical field H_c is a root mean square value of the induction at H_{c2} . Having exact sense for thick type-I superconductors [2, 15], this side of H_c was not known for type-II materials.

Therefore, the vortex matter in samples of the transverse geometry can be viewed as a peculiar 2D ideal gas where a role of pressure P is taken by the applied field H and the equation of state is given by Eq. (3).

Indeed, similar to the gas, which isothermal compressibility $\rho^{-1}(\partial\rho/\partial P)_T = 1/P$ (ρ is the gas density), the vortex gas is highly compressible and its “compressibility” $n^{-1}(\partial n/\partial H)_T = 1/H$. Similar to the gas, where the slope of ρ vs P is determined by the Boltzmann constant, in the “vortex gas” the slope of n vs H is determined by the fundamental constant Φ_0 . But, contrary to the gas, properties of the vortex matter do not depend on temperature. Therefore vortices in the slab in the perpendicular field can be treated as a gas at zero temperature and hence with zero entropy, which makes this gas ordered.

Comparing the gas-like scenario with solid-like pictures [18, 32], one can see that the former is more appropriate for the vortex matter since a primary property of solids, rigidity, is absent in the vortex ensemble. Extending this analogy, the vortex matter in samples with $\eta \neq 1$ can be viewed as a “real gas”, where interactions are the most significant for $\eta = 0$.

Finally, the near-surface inhomogeneities, like in the Peierls-London model, are not included in our model of the zero-order approximation. But, contrary to the IS, where effects of these inhomogeneities were noticed already in 2 mm thick samples [33], such effects were not found in the reported experiments. This can be explained by a finer pattern of these inhomogeneities (compare images in Fig. 6 with those in [26]) and by the absence of the factor of symmetry in the IS, leading to the condition $H_{c2\perp} = H_{c2\parallel}$ in the MS. Therefore, the surface effects in the MS can be expected in thinner samples and they should differ from those in the IS, hence constituting an important problem of fundamental superconductivity.

SUMMARY AND OUTLOOK

Equilibrium properties of the mixed state in type-II superconductors were studied with high purity bulk and film niobium samples with zero and unity demagnetizing factor η . A magnetization curve of the samples with $\eta=1$ was obtained for the first time. It was found that existing theories are not capable to describe these new data. A theoretical model successfully addressing this problem was developed and experimentally validated.

The new model describes magnetic properties of the mixed state in a zero order approximation where interactions between vortices are ignored. It is applicable to samples with any η without limitation in magnitude of the Ginzburg-Landau parameter κ . The model is quantitatively consistent with the data obtained for the samples with $\eta = 1$, thus indicating that the interaction between vortices in such case is vanishing. A new formula for the

line tension of vortices valid in the entire field range of the mixed state is obtained. It is shown that the root mean square value of the induction at the applied field $H \rightarrow H_{c2}$ is the thermodynamic critical field H_c . At low κ the model converts to that of Peierls and London for the intermediate state in type-I superconductors, valid in the limit of non-interacting laminae.

It is shown, that visualization of the vortex matter as an ordered 2D gas at zero temperature is more appropriate than frequently used solid-like scenarios. Since the vortices in the samples with $\eta = 1$ do not interact, the “vortex gas” in such samples is ideal. For $\eta \neq 1$ accounting for the vortex interaction is important for the description of the magnetic properties beyond the zero-order approximation.

It is shown that effects of the surface related inhomogeneities differ from those in the intermediate state in type-I superconductors, but specific form of these effects remain to be revealed. Investigation of these effects is important for further progressing in understanding properties of type-II superconductors.

Acknowledgments

We express a deep gratitude to Michael E. Fisher for reading and commenting on manuscript, and to Oscar Bernal and Andrew MacFarlane for the crucial help in organizing the project. This work was supported in part by the National Science Foundation (Grant No. DMR 0904157), by the Research Foundation – Flanders (FWO, Belgium) and by the Flemish Concerted Research Action (BOF KU Leuven, GOA/14/007) research program.

- [1] L. V. Shubnikov, V. I. Khotkevich, Yu. D. Shepelyev, Yu. N. Ryabinin, *Zh.E.T.F.* **7**, 221 (1937).
- [2] D. Shoenberg, *Superconductivity*, 2nd. ed., (Cambridge University Press, 1952).
- [3] B. Serin, in *Superconductivity*, v. 2, Ed. R. D. Parks (Marcel Dekker, Inc., N.Y., 1969).
- [4] E. H. Brandt, *Rep. Prog. Phys.* **58**, 1465 (1995).
- [5] J. C. Maxwell, *A Treatise on Electricity and Magnetism*, v.II, 2nd ed. (Oxford, Clarendon Press, 1881).
- [6] P. G. De Gennes, *Superconductivity of Metals and Alloys* (Perseus Book Publishing, L.L.C., 1966).
- [7] A. A. Abrikosov, *Fundamentals of the Theory of Metals* (Elsevier Science Pub. Co., 1988).
- [8] L. D. Landau, E.M. Lifshitz and L. P. Pitaevskii, *Electrodynamics of Continuous Media*, 2nd ed. (Elsevier, 1984).
- [9] R. Peierls, *Proc. Roy. Soc. London, Ser. A* **155**, 613 (1936).
- [10] F. London, *Physica* **3**, 450 (1936);
- [11] F. London, *Superfluids* v. 1, 2nd ed. (Dover, N.Y., 1961).

- [12] A. A. Abrikosov, Zh.E.T.F. **32**, 1442 (1957) [Sov. Phys. JETP **5**, 1174 (1957)].
- [13] J. D. Livingston, Phys. Rev. **129**, 1943 (1963).
- [14] D. K. Finnemore, T. F. Stromberg, C. A. Swenson, Phys. Rev. **149**, 231 (1966).
- [15] V. Kozhevnikov and C. Van Haesendonck, Phys. Rev. B **90**, 104519 (2014).
- [16] L. P. Gor'kov, Zh.E.T.F. **36**, 1918 (1959) [Sov. Phys. JETP **36**(9), 1364 (1959)].
- [17] E. M. Lifshitz and L. P. Pitaevskii *Statistical Physics* v.2, M., Nauka, 1973.
- [18] M. Tinkham, *Introduction to Superconductivity* (McGraw-Hill, 1996).
- [19] H. Koppe and J. Willebrand, J. Low-Temp. Phys. **2**, 499 (1970).
- [20] E. R. Andrew and J. M. Lock, Proc. Phys. Soc. A **63**, 13 (1949).
- [21] P. B. Miller, B. W. Kington, D. J. Quinn, Rev. Mod. Phys. **36**, 70 (1964).
- [22] G. D. Cody and R. E. Miller, Phys. Rev. **173**, 481 (1968).
- [23] A. L. Fetter and P. C. Hohenberg, in *Superconductivity*, v. 2, Ed. R. D. Parks (Marcel Dekker, Inc., N.Y., 1969).
- [24] E. H. Brandt, Phys. Rev. B **71**, 014521 (2005).
- [25] M. M. Doria, E. H. Brandt and F. M. Peeters, Phys. Rev. B **78**, 054407 (2008).
- [26] V. Kozhevnikov, R. J. Wijngaarden, J. de Wit, and C. Van Haesendonck. PRB **89**, 100503(R) (2014).
- [27] A. Maisuradze, A. Yaouanc, R. Khasanov, A. Amato, C. Baines, D. Herlach, R. Henes, P. Keppler, and H. Keller, PRB **88**, 140509(R) (2013).
- [28] G. Wu, A.-M. Valente, H.L. Phillips, H. Wang, A.T. Wu, T.J. Renk, P. Provencio, Thin Solid Films **489**, 56 (2005).
- [29] Anne-Marie Valente-Feliciano. Development of SRF monolayer/multilayer thin film materials to increase the performance of SRF accelerating structures beyond bulk Nb. PhD dissertation, Universit Paris Sud - Paris XI, 2014.
- [30] A. Oral, S. J. Bending and M. Henini, Appl. Phys. Lett. **69**, 1324 (1996).
- [31] A. F. Andreev, Zh.E.T.F. **51**, 1510 (1966).
- [32] G. Blatter, M. Y. Feigel'man, Y. B. Geshkenbein, A. I. Larkin, V. M. Vinokur, Rev. Mod. Phys. **66**, 1125 (1994).
- [33] Yu. V. Sharvin, Zh.E.T.F. **33**, 1341 (1957) [Sov. Phys. JETP **33**, 1031 (1958)].